Supplemental Data

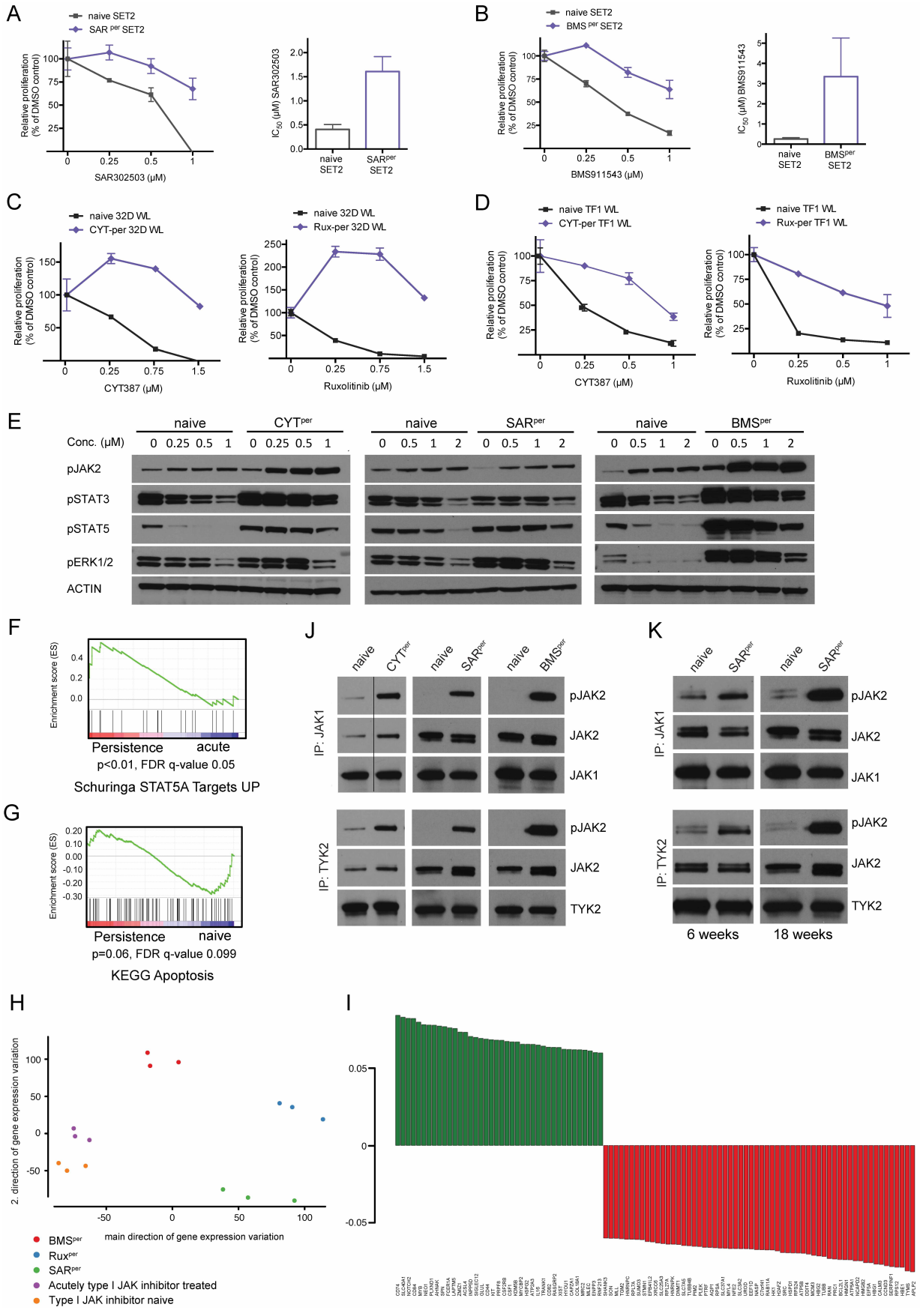

L

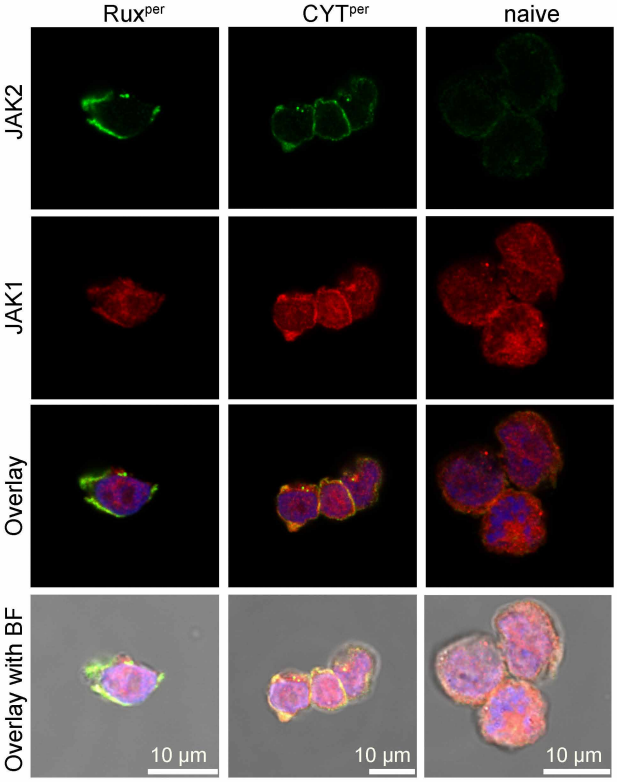

M

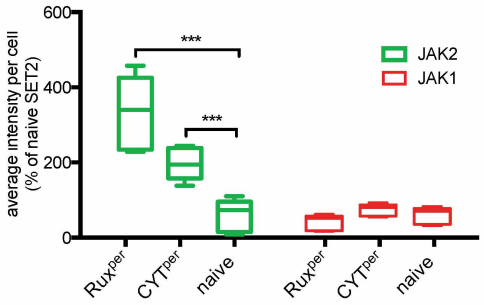

N

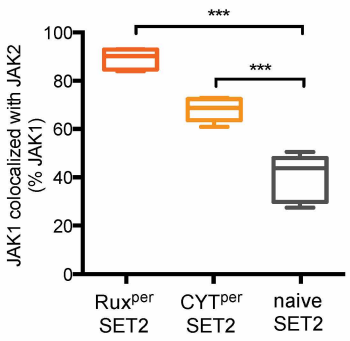

O

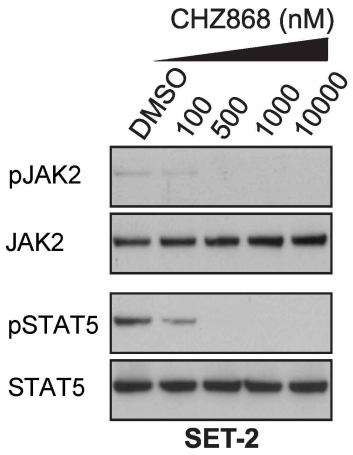

P

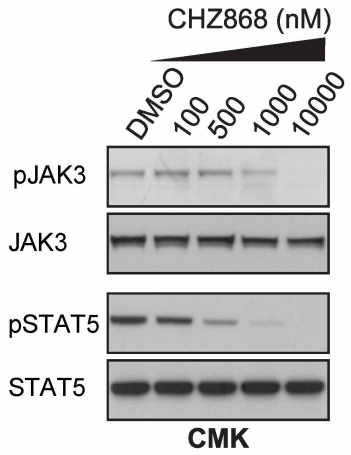

Q

Cell proliferation assays

Cell line	GI_{50} (nM)
SET-2 $JAK2^{V617F}$	59
CMK $JAK3^{A572V}$	378
K562 BCR-ABL	4627

R

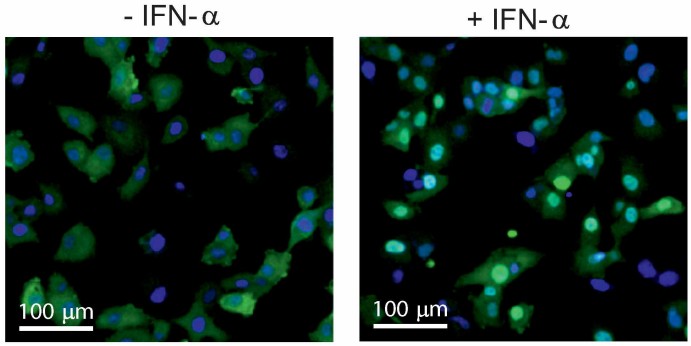

S

Cellomics STAT1-GFP translocation assay

Compound	IC_{50} (nM)
tofacitinib	7.4 ± 1.6
CHZ868	482 ± 163

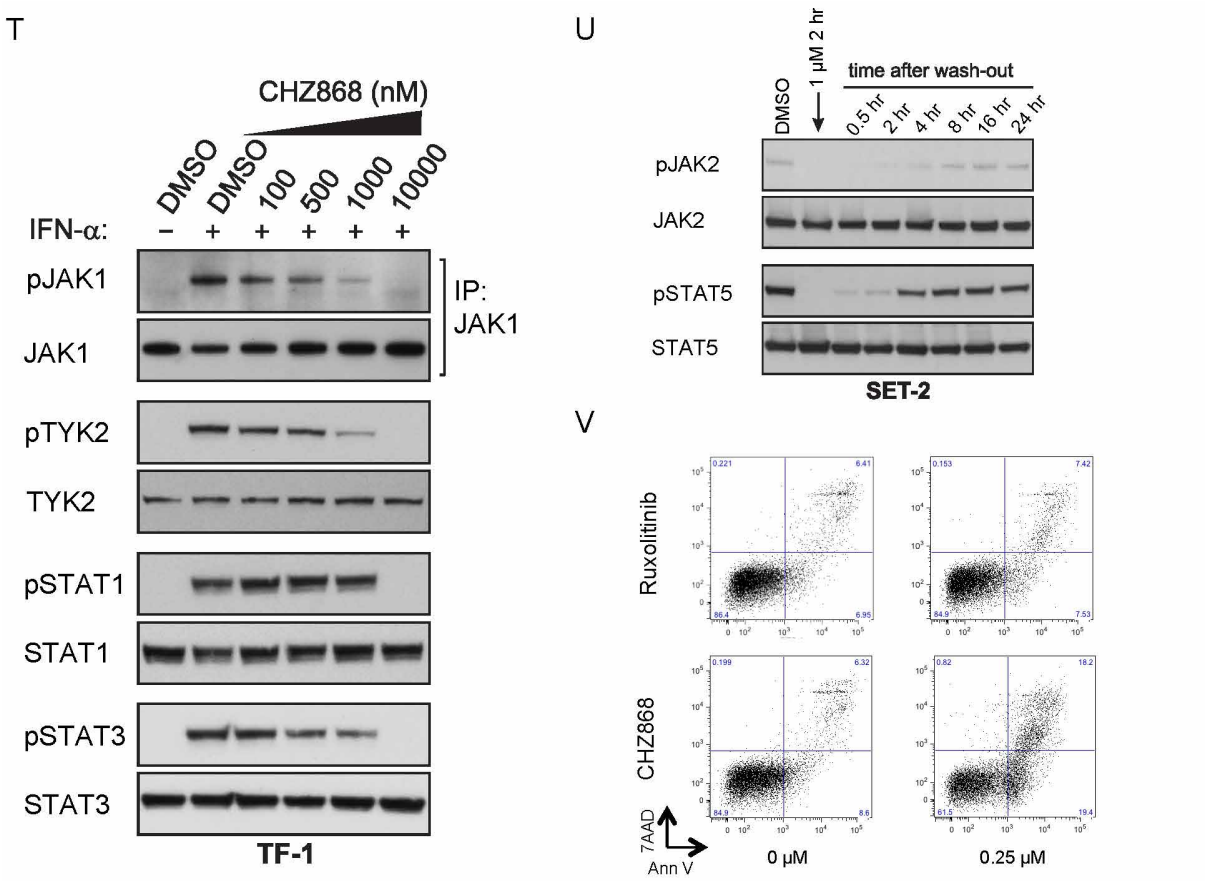

Figure S1, Related to Figure 1. Persistence to type I JAK inhibitors and profiling of type II JAK inhibition by CHZ868. A-B. Proliferation with increasing concentrations of SAR302503 or BMS911543 (μM) relative to proliferation in the presence of DMSO as control is shown for naive SET2 cells and for SET2 cells chronically cultured in the presence of SAR302503 (SAR^{per} SET2) or BMS911543 (BMS^{per} SET2, left panels), respectively. IC_{50} values for SAR302503 and BMS911543 in naive, SAR^{per} and BMS^{per} SET2 are indicated in the right panels. All data are represented as mean ± SEM. **C.** Proliferation with increasing concentrations of CYT387 or ruxolitinib (μM) relative to proliferation in the presence of DMSO is shown for naive 32D *MPL*W515L cells and for 32D *MPL*W515L cells chronically cultured in the presence of CYT387 (CYT^{per} 32D WL) or ruxolitinib (Rux^{per} 32D WL). Data are represented as mean ± SEM. **D.** CYT387 and ruxolitinib are analogously assessed in naive TF1 *MPL*W515L cells and in TF1 *MPL*W515L cells chronically cultured in the presence of CYT387 (CYT^{per} TF1 WL) or ruxolitinib (Rux^{per} TF1 WL). Data are represented as mean ± SEM. **E.** Phosphorylation of JAK2, STAT3, STAT5 and ERK1/2 is assessed in naive SET2 as compared to CYT^{per}, SAR^{per} and BMS^{per} SET2 upon 4 hr exposure to CYT387, SAR302503 or BMS911543, respectively. **F.** The STAT5

gene expression signature as described by Schuringa et al(Schuringa et al., 2004) is evaluated for enrichment by gene set enrichment analysis (GSEA) in type I JAK inhibitor persistent cells vs. acute ruxolitinib treatment. **G.** The apoptosis gene expression signature as described by KEGG is evaluated for enrichment by GSEA in type I JAK inhibitor persistence compared to naive cells. **H.** Principal component analysis (PCA), which separates differential gene expression data according to the most variance along a first (main) and a second direction of gene expression variation, is shown for the several type I JAK inhibitor persistent cells as compared to naive cells and to acute ruxolitinib treatment. **I.** The top 100 genes with the highest variation in gene expression between type I JAK inhibitor persistent cells and naive or acutely ruxolitinib-treated cells, which lead to separation of samples along the main axis of variation by PCA in Figure S1H, are indicated. **J.** Phosphorylation of JAK2 co-immunoprecipitated with JAK1 (upper panel) and TYK2 (lower panel) is shown in naive as well as in CYT^{per}, SAR^{per} and BMS^{per} SET2 cells. Immunoprecipitates of JAK1 from naive vs. CYT^{per} cells were run in non-adjacent lanes of the same gel. **K.** JAK2 phosphorylation in co-immunoprecipitates with JAK1 (upper panel) and TYK2 (lower panel) is assessed in SAR^{per} SET2 cells at 6 weeks and at 18 weeks of continuous culture with SAR302503 as compared to naive SET2 cells. **L.** Immunofluorescent double staining for JAK2 (green) and JAK1 (red) is shown in naive vs. CYT387 and ruxolitinib persistent SET2 cells. Overlay of JAK2 and JAK1 immunofluorescent staining (yellow) reflects co-localization of JAK2 and JAK1. Overlay of immunofluorescent double-staining with bright field (BF) visualizes the localization of JAK2 and JAK1 relative to the cell surface. **M.** Quantitation of average fluorescence intensities per cell reflecting JAK2 and JAK1 expression levels is shown in naive vs. CYT387 and ruxolitinib persistent SET2 cells. Box and whiskers plots indicate medians (central line) with 25^{th} and 75^{th} percentile (box boundaries), with whiskers showing minimum and maximum values (***$p<0.001$ versus naive SET2 cells). **N.** Co-localization analysis was performed on naive vs. CYT387 and ruxolitinib persistent SET2 cells by Metamorph software after thresholding the fluorescence intensities of each protein. Box and whiskers plots indicate medians (central line) with 25^{th} and 75^{th} percentile (box boundaries), with whiskers showing minimum and maximum values (***$p<0.001$ versus naive SET2 cells). **O-P.** Phosphorylation of JAK2 and STAT5 upon 1 hr exposure to increasing concentrations of CHZ868 in *JAK2*V617F-positive SET2 cells and in *JAK3*V572A-positive CMK cells**. Q.** Half-maximal growth inhibitory concentrations (GI_{50}) as determined in cell proliferation assays with CHZ868 using *JAK2*V617F mutant, *JAK3*V572A mutant and *BCR-ABL* rearranged cells. GI_{50} values represent means of two independent experiments. **R.** Representative composite images of HT1080 fibrosarcoma cells stably expressing STAT1-GFP at baseline (left panel) and after stimulation with 100 ng/ml IFN-α for 30 min (right panel). **S.** IC_{50} values determined in the IFN-α mediated STAT1-GFP nuclear translocation assay for CHZ868 as compared to the pan-JAK

inhibitor tofacitinib (means of 3 independent experiments ± SD). **T.** TF-1 cells starved in GM-CSF deficient media for 4 hr and pre-treated with CHZ868 or DMSO for 1 hr were stimulated with 20 ng/ml INF-α for 10 min and the effect of increasing concentrations CHZ868 on phosphorylation of JAK1, TYK2 and STAT3 is shown by Western blotting. **U.** JAK-STAT signaling in *JAK2*V617F SET2 cells after 2 hr exposure to CHZ868 (1 μM), followed by compound wash-out. **V.** Induction of apoptosis as reflected by Annexin V and 7AAD positivity upon 24 hr incubation with CHZ868 or ruxolitinib.

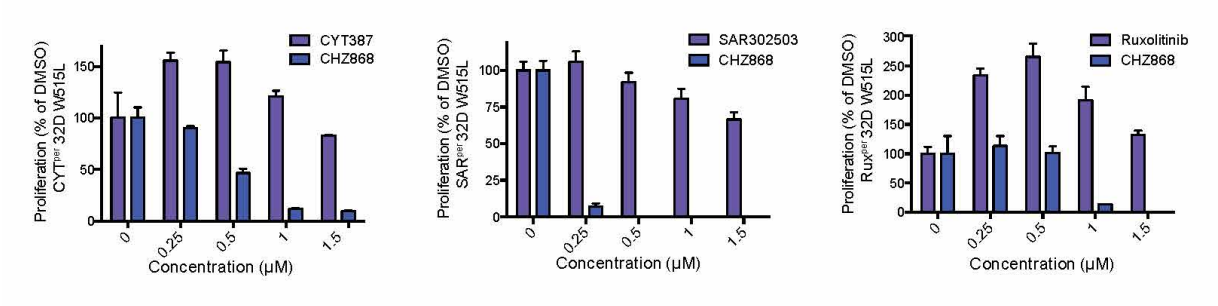

Figure S2, related to Figure 2. Effect of CHZ868 on type I JAK inhibitor persistent cells in vitro. Proliferation of CYT387 (CYT^{per}), SAR302503 (SAR^{per}) and ruxolitinib (Rux^{per}) persistent 32D *MPL*W515L cells upon increasing concentrations of the respective type I JAK inhibitor or CHZ868 relative to proliferation in presence of DMSO. Data are represented as mean ± SEM.

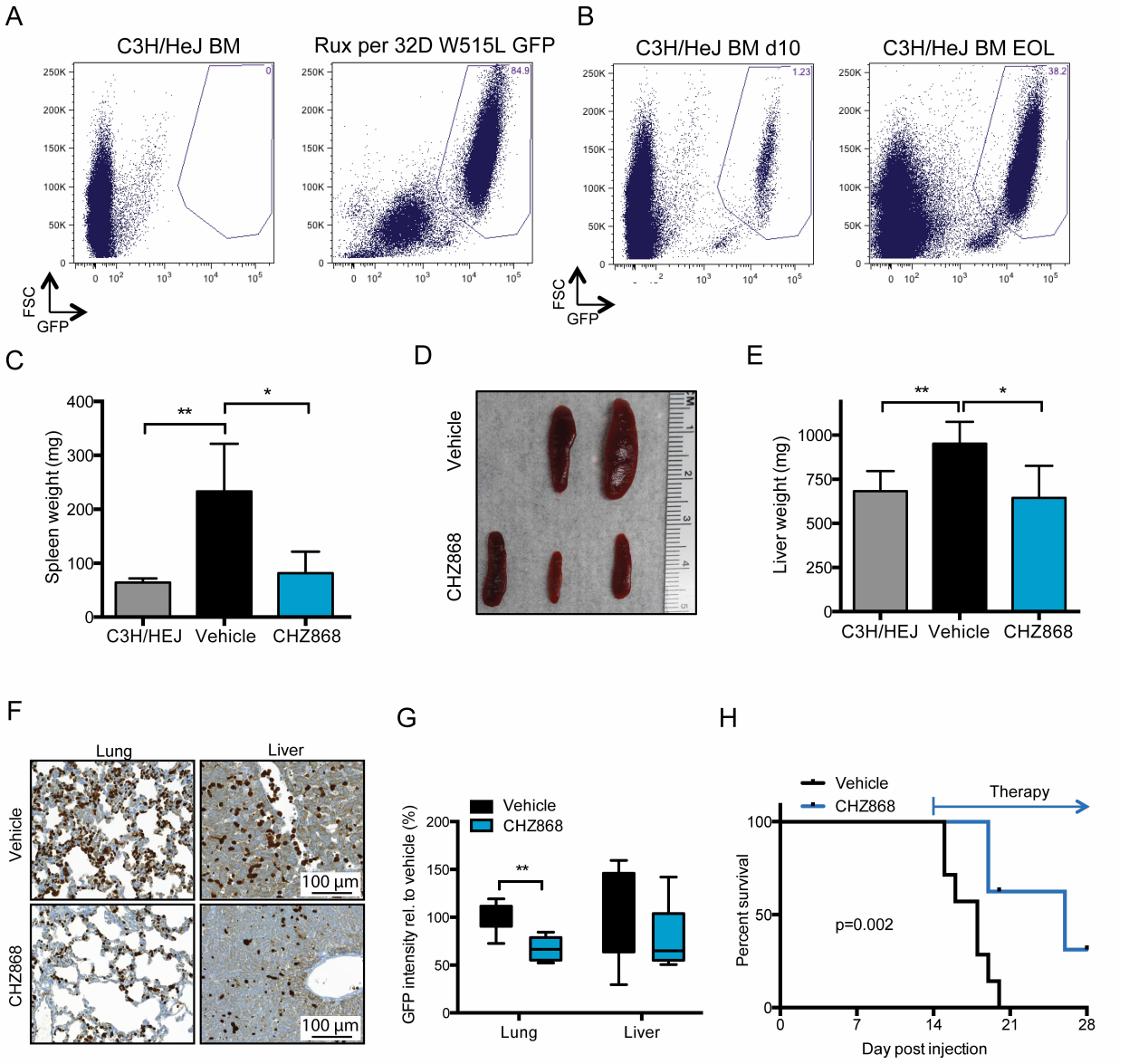

Figure S3, related to Figure 3. Effect of CHZ868 on ruxolitinib persistent 32D *MPL*W515L GFP$^+$ cells in vivo. A. Flow cytometric analysis for GFP in bone marrow (BM) of normal C3H/HeJ mice or in vitro cultured Rux^{per} 32D *MPL*W515L GFP$^+$ cells. **B.** Flow cytometric analysis for GFP in bone marrow of C3H/HeJ mice transplanted with Rux^{per} 32D *MPL*W515L GFP$^+$ cells 10 days after injection (d10) and at end of life (EOL). **C-D.** Spleen weight and size of C3H/HeJ mice transplanted with Rux^{per} 32D *MPL*W515L GFP$^+$ cells, after 7 days of treatment with CHZ868 at 40 mg/kg or with vehicle. Spleen weight of age-matched control C3H/HeJ mice is also indicated. Spleen weights are represented as mean ± SEM (*p<0.05, **p<0.01 versus vehicle group). **E.** Liver weight of C3H/HeJ mice transplanted with Rux^{per} 32D *MPL*W515L GFP$^+$ cells, after 7 days CHZ868 at 40 mg/kg vs. vehicle treatment. Liver weight of age-matched control C3H/HeJ mice is also indicated. Data are represented as mean ± SEM (*p<0.05, **p<0.01 versus vehicle group). **F.** Immunohistochemistry staining for GFP in lung and liver of

C3H/HeJ mice transplanted with Rux^{per} 32D *MPL*W515L GFP^+ cells after treatment with CHZ868 40 mg/kg or vehicle visualizes the extent of organ infiltration by Rux^{per} 32D *MPL*W515L GFP^+ cells**. G.** Quantitation of 32D *MPL*W515L GFP^+ infiltration upon treatment with CHZ868 40 mg/kg or vehicle using Metamorph software after color thresholding. Box and whiskers plots indicate medians (central line) with 25^{th} and 75^{th} percentile (box boundaries), with whiskers showing minimum and maximum values (**$p<0.01$ versus vehicle group). **H.** Survival curve of C3H/HeJ mice transplanted with Rux^{per} 32D *MPL*W515L GFP^+ cells. In vivo disease by Rux^{per} 32D *MPL*W515L cells is lethal within 20 days after injection. Treatment with CHZ868 significantly prolongs survival ($p=0.002$) with 25% of CHZ868 treated mice alive at 2 weeks of therapy, when the studies were concluded. Results are representative of 2 independent studies.

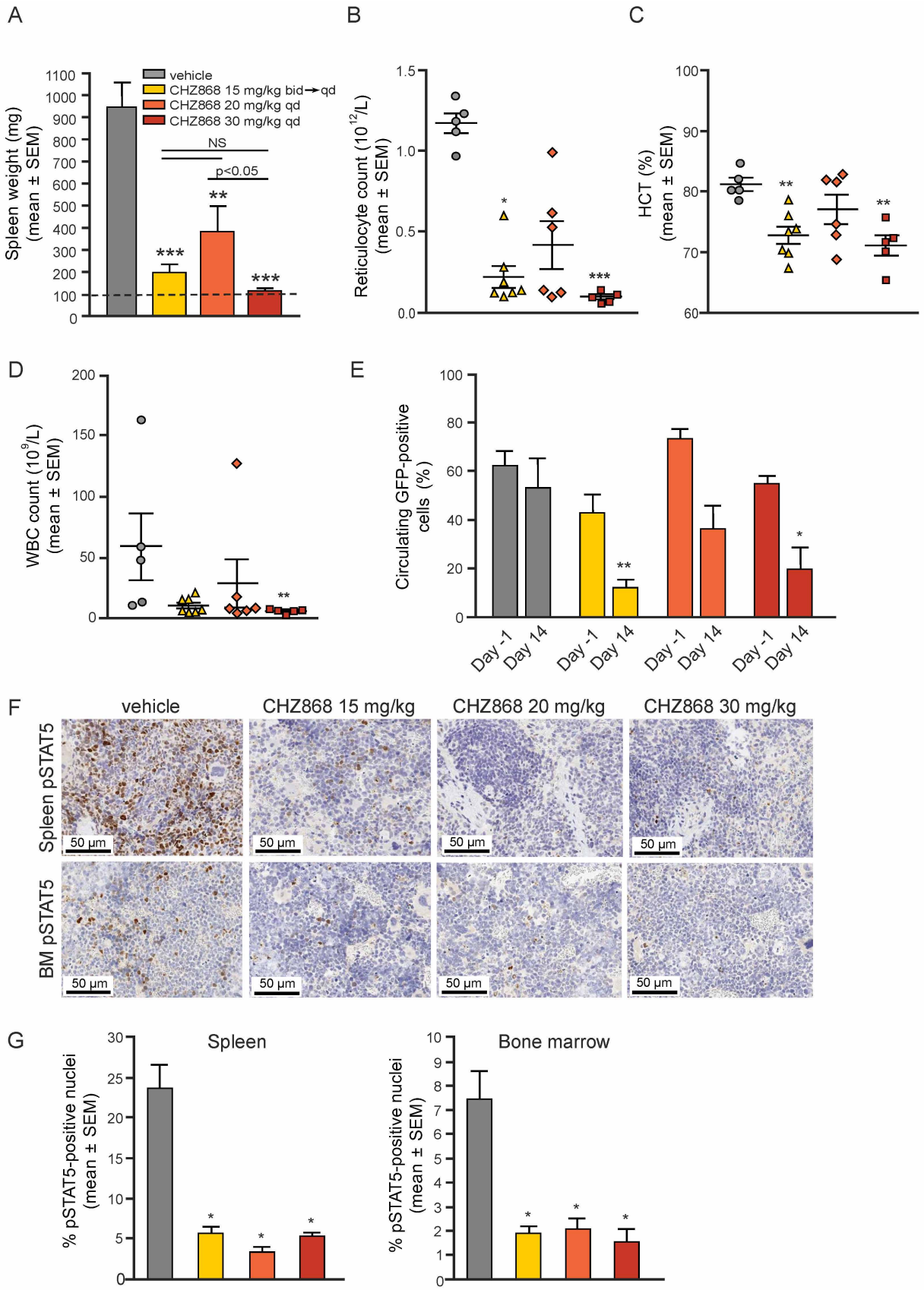
A
B
C
vehicle
CHZ868 15 mg/kg bid→qd
CHZ868 20 mg/kg qd
CHZ868 30 mg/kg qd
NS
p<0.05
Spleen weight (mg)
(mean ± SEM)
Reticulocyte count (10^12/L)
(mean ± SEM)
HCT (%)
(mean ± SEM)
D
E
WBC count (10^9/L)
(mean ± SEM)
Circulating GFP-positive cells (%)
Day -1
Day 14
F
vehicle
CHZ868 15 mg/kg
CHZ868 20 mg/kg
CHZ868 30 mg/kg
Spleen pSTAT5
BM pSTAT5
50 µm
G
Spleen
Bone marrow
% pSTAT5-positive nuclei
(mean ± SEM)

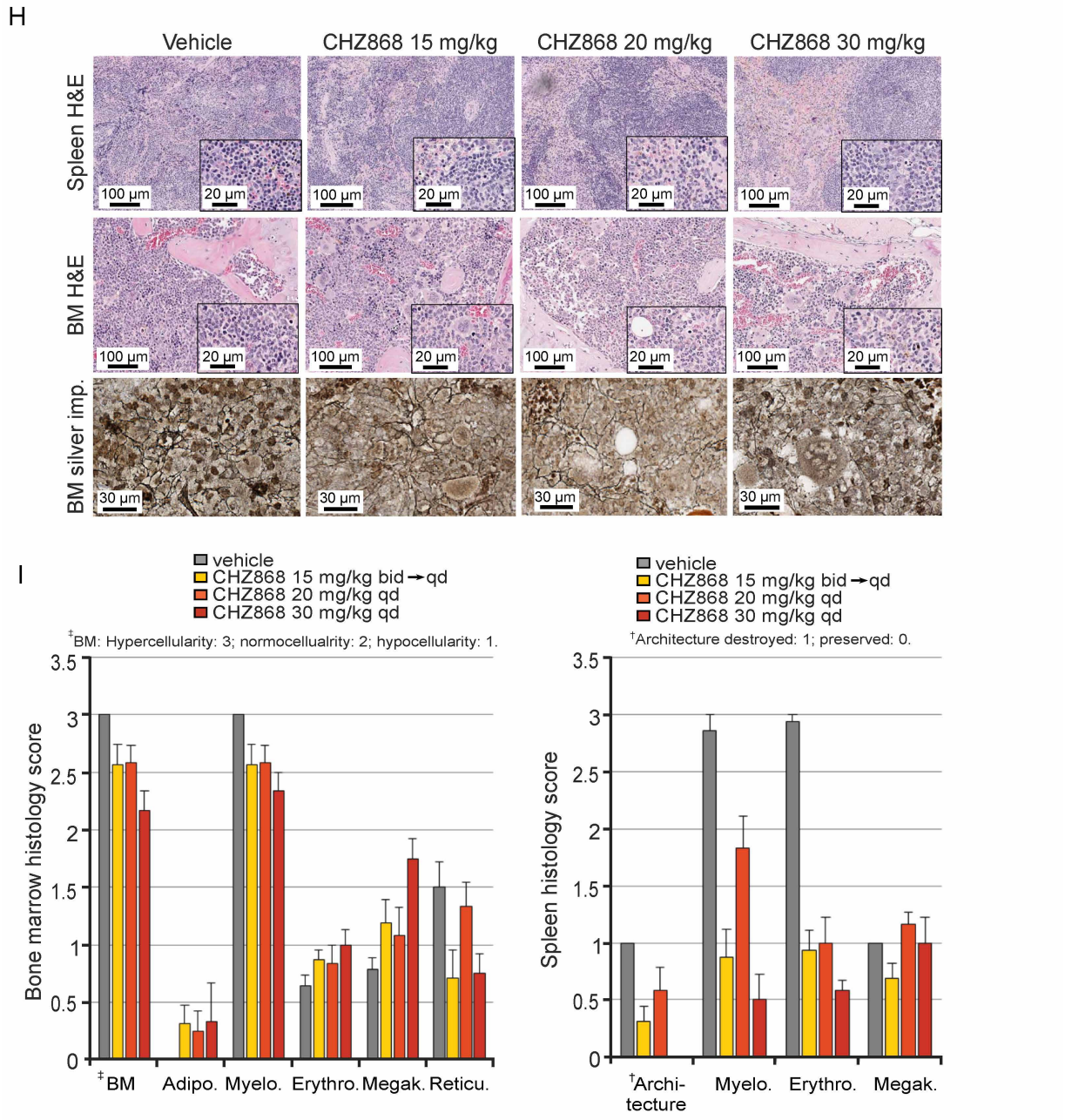

Figure S4, Related to Figure 4. Type II JAK inhibition by CHZ868 in vivo in the *Jak2*V617F retroviral bone marrow transplant model of MPN. A. Spleen weight in the *Jak2*V617F retroviral transplant model after 2 weeks of treatment with CHZ868 15 mg/kg bid for one week and then qd, 20 mg/kg qd, 30 mg/kg qd or vehicle. Data are represented as means ± SEM, n=6-8/group). Stippled line depicts normal spleen weight from age-matched non-transplanted BALB/c mice (98 mg). **p<0.01 or ***p<0.001 versus vehicle group; One-way ANOVA on $\log_{10}$ transformed values followed by Dunnett's test. Reticulocyte count **(B)**, HCT **(C)**, and WBC count **(D)** post-therapy (Data represented as means ± SEM, n=5-7 available samples per group, missing values due to technical issues). Grey circles: vehicle; yellow triangles: 15 mg/kg

CHZ868 (bid schedule changed to qd after 1 week of dosing); orange diamonds: 20 mg/kg CHZ868 qd; red squares: 30 mg/kg CHZ868 qd. *p<0.05, **p<0.01 or ***p<0.001 versus vehicle group. Statistical analysis was done by ANOVA on ranks followed by Dunn's test for reticulocyte count, and by one-way ANOVA followed by Dunnett's test for HCT and WBC count (1/x transformed values for the latter parameter). **E.** Mutant allele burden in the *Jak2*V617F transplant model as reflected by the percentage of GFP^+ cells (of total nucleated cells) in circulation assessed one day prior to start and at 2 weeks of treatment with CHZ868. Results are depicted as means ± SEM (analysis on n=5-8 available samples per group, missing values due to technical issue). Color code of bars in the histogram corresponds to panel A. *p<0.05, or **p<0.01 versus vehicle group; One-way ANOVA followed by Dunnett's test. **F-G.** Representative immunohistochemistry images of spleen and bone marrow in the *Jak2*V617F transplant model stained for pSTAT5 after 14 days of treatment with CHZ868 or vehicle. Quantification in spleen and bone marrow sections using the Definiens image analysis software. Color code of bars in the histogram corresponds to panel A. Results are depicted as means ± SEM (n=6-8 per group). *p<0.05 versus vehicle group; One-way ANOVA followed by Dunn's test. **H.** Representative H&E images of spleen and bone marrow for assessment of myelo-erythroid infiltration in spleen and cellularity of bone marrow after treatment with CHZ868 or vehicle in the *Jak2*V617F transplant model. Representative silver impregnation stainings of bone marrow show reticulin fibers as fine black streaks. **I.** Quantification of bone marrow hypercellularity and reticulin fibrosis by bone marrow histology score (left panel, data represented as mean ± SEM, n=6-8 samples per group) and quantification of myelo-erythroid infiltration in the spleen by spleen histology score (right panel, data represented as mean ± SEM). Abbreviations: Myeloid cells (Myelo), erythroid cells (Erythro), megakaryocytes (MK), adipocytes (Adipo) and reticulin (Reticu).

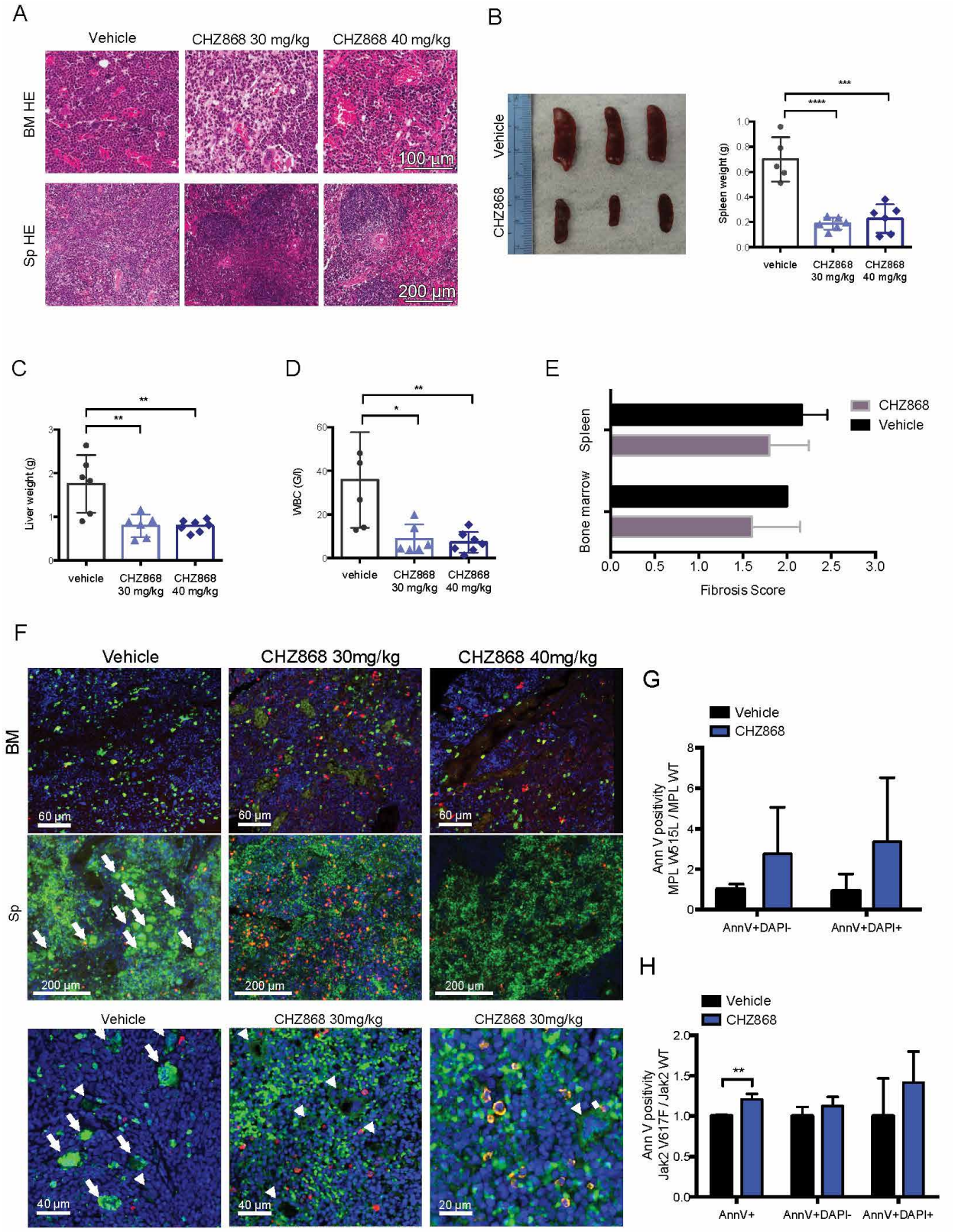

Figure S5, Related to Figure 5. Type II JAK inhibition by CHZ868 in vivo in the *MPL*W515L retroviral bone marrow transplant model of MPN. A. Representative H&E images from bone marrow and spleen of the *MPL*W515L transplant model reflecting the extent of hypercellularity

after treatment with CHZ868 or vehicle. **B-D.** Spleen size and weight, liver weight and peripheral blood white blood cell counts (WBC) in *MPL*W515L induced myelofibrosis in C57BL/6 mice upon 3 weeks treatment with CHZ868 vs. vehicle. Data are represented as mean ± SEM (*p<0.05, **p<0.01, ***p<0.001 or ****p<0.0001 versus vehicle group). **E.** Quantitation of reticulin fibrosis in the *MPL*W515L transplant model using spleen and bone marrow fibrosis scores. Data are represented as mean ± SEM. **F.** Immunofluorescencent staining for *MPL*W515L GFP^+ hematopoietic cells (green) and cleaved Caspase-3 (red) reflecting apoptosis in bone marrow (BM, top row) and spleen (Sp, middle row) of the *MPL*W515L model after 10 days of treatment with CHZ868. Double-positive cells (yellow) represent GFP positive, cleaved Caspase-3 positive cells. At higher magnification (bottom row), *MPL*W515L GFP^+ megakaryocytes are depicted by arrows and *MPL* WT GFP^- megakaryocytes by arrowheads. **G.** Flow cytometric analysis for annexin V positivity in the *MPL*W515L model after 10 days of treatment with CHZ868 40 mg/kg focusing on apoptosis induction in *MPL*W515L vs. WT Lin^- $Sca1^-Kit^+$ multipotent myeloid progenitors. Annexin V^+ $DAPI^-$ cells are considered early apoptotic, Annexin V^+ $DAPI^+$ cells are considered late apoptotic. Data are represented as mean ± SEM. **H.** Flow cytometric analysis for annexin V positivity in $Lin^-Sca1^-Kit^+$ multipotent myeloid progenitors of mice competitively transplanted with *Jak2*V617F CD45.2 and *Jak2* WT CD45.1 bone marrow and treated with CHZ868 for 2 days. Induction of apoptosis is determined in *Jak2*V617F vs. *Jak2* WT multipotent myeloid progenitors (Annexin V^+: total apoptotic progenitor cells, Annexin V^+ $DAPI^-$: early apoptotic progenitor cells, Annexin V^+ $DAPI^+$: late apoptotic progenitor cells). Data are represented as mean ± SEM (**p<0.01 versus vehicle group).

Supplemental Experimental Procedures

Transcriptional profiling, gene set enrichment analysis (GSEA) and principal component analysis (PCA). After cell lysis in TRIzol (Life Technologies), whole transcriptome sequencing was performed on Proton. After ribogreen quantification and quality control on Agilent BioAnalyzer (RIN>8), poly(A) RNA was isolated using Dynabeads® mRNA DIRECT™ Micro Kit (Life Technologies) from 1 µg of total RNA. mRNA was then fragmentated using RNaseIII and purified. The fragmented samples' quality and yield were evaluated using Agilent BioAnalyzer. Subsequently, the fragmented material underwent whole transcriptome library preparation according to the Ion Total RNA-Seq Kit v2 protocol (Life Technologies), with 16 cycles of PCR. Samples were barcoded, template-positive Ion PI™ Ion Sphere™ Particles (ISPs) were prepared using the ion one touch system II and Ion PI™Template OT2 200kit v2 Kit (Life Technologies). Enriched particles were sequenced on a Proton sequencing system using 200 bp version 2 chemistry. An average of 42 million reads per sample were generated. To process the raw sequencing data for gene expression counting and differential analysis, the RAW output BAMs were converted to FASTQ using PICARD Sam2Fastq. Then the reads were first mapped to the human genome using rnaStar. The genome used was HG19 from UCSC with junctions from ENSEMBL (Homo_sapiens.GRCh37.69_ ENSEMBL) and a read overhang of 49. Any unmapped reads were mapped again to HG19 using BWA MEM (version 0.7.5a). The two mapped BAMs were then merged and sorted and gene level counts were computed using htseq-count (options -s y -m intersection-strict) and the same gene models used in the rnaStar mapping step (Homo_sapiens.GRCh37.69_ENSEMBL). Differential gene expression was assessed in type I JAK inhibitor persistent cells vs. naïve cells or vs. acute ruxolitinib treatment. To evaluate enrichment of STAT5 and apoptosis related gene sets, we applied GSEA(Subramanian et al., 2005), a computational method determining whether *a priori* defined gene sets show statistically significant differences between two biological datasets. We first applied VOOM(Law et al., 2014) to transform and normalize the RNA-seq read count distribution into a normal-based microarray-like distribution, as GSEA is designed for microarray data. Signature gene sets were extracted from the Molecular Signature Database, version 4 (MSigDBv2)(Subramanian et al., 2005). For STAT5A target gene analysis, the experimentally defined STAT5 signature reported by Schuringa et al(Schuringa et al., 2004) was used. The apoptosis gene signatures used were previously reported by Alcala et al(Alcala et al., 2008) and by the Kyoto Encyclopedia of Genes and Genomes (KEGG). Enrichment with a p value <0.05 and an FDR q-value <0.25 was considered statistically significant. In addition, we applied PCA on the 1000 genes with the most variance in expression in order to extract the main directions of variation in gene expression between type I inhibitor persistent cells, naive cells and acute

ruxolitinib treatment. PCA is a classical technique(Jolliffe, 2002) that reveals inherent data structure by projecting the data on a lower dimensional space. Namely, PCA uses eigenvector decomposition to extract orthogonal directions (also called Principal Components, PC) such that the k-th PC captures the k-th most variance along the PCs. Here, we evaluated the projection of the samples on the first two PCs, i.e. the first and second direction of gene expression variation.

Immunofluorescence for JAK heterodimers. Naive and type I inhibitor persistent SET2 cells were fixed in 4 % paraformaldehyde, blocked in PBS/0.3 % Triton X 100/5 % goat serum and stained overnight for JAK2 (CST) and JAK1 (BD) at 1:100 dilution. Goat anti-rabbit Alexa488 and goat anti-mouse Alexa594 (Invitrogen) were used as secondary antibodies at 1:200 dilution. Cells were stained with DAPI 0.5 µg/ml and mounted in Mowiol mounting media. Confocal immunofluorescence images were acquired with a Leica TCS SP5-II upright microscope using a 63X lens (NA.1.4 HCX PL APO). Excitation lines of 405nm, 488nm, and 594nm were used to capture DAPI, JAK1 and JAK2, respectively, and a bright field image was taken for visualization of cell membrane. Same laser powers were kept to image all cells for objective image analysis using Metamorph software (Molecular Devices). Average cellular intensities of JAK1 and JAK2 were calculated by measuring the integrated intensity divided by the number of cells in each image. For colocalization analysis of JAK1 and JAK2 proteins, Measure Colocalization application in Metamorph software was used after thresholding each protein.

Supplemental cell lines and signaling analyses. *JAK3*A572V mutant CMK cells (DSMZ) were grown in RPMI1640/20% FCS and K562 cells (ATCC, Manassas, VA) in RPMI1640/10% FCS and 2 mM L-glutamine. TF-1 cells (ATCC, Manassas, VA, USA) were cultured in RPMI/10 % FCS, 1 mM L-glutamine, 1 mM sodium pyruvate, 1.5 g/l sodium bicarbonate, 10 mM HEPES, 2 ng/ml GM-CSF. To assess inhibition of IFN-α signaling, TF-1 cells were starved in the absence of GM-CSF for 4 hr and then pre-treated with increasing concentrations of CHZ868 or with DMSO for 1 hr. Cells were stimulated with 20 ng/mL IFN-α for 10 min, followed by extraction. JAK1 was immunoprecipitated from 500 µg total cell lysate (BD) followed by Western blot detection of phospho-JAK1 (Tyr1022/Tyr1023, Abcam). HT1080 fibrosarcoma cells (ATCC, Manassas, VA, USA) stably expressing STAT1-GFP were cultured in MEM α/10 % FCS/400 µg/ml geneticin.

IFN-α mediated STAT1-GFP nuclear translocation assay. STAT1 cDNA (GenBank accession number NM_007315) was obtained from LGC Promochem and PCR amplification performed using PCR primers STAT1-F GTG GAC CAG CTG AAC ATG TTG G and STAT1-REco GAA TTC CAC TTC AGA CAC AGA AAT CAA CTC AGT C (Microsynth, Balgach,

Switzerland) using Taq Polymerase (Sigma-Aldrich, St. Louis, MO, USA). The expected size 597bp fragment comprising the carboxy terminus of STAT1 was Topo-TA cloned into pCDNA3.1 Topo TA-His (Life Technologies, Carlsbad, CA, USA) following the manufacturers' instructions. Subsequent to sequence confirmation, the fragment was digested *Hind*III-*Eco*R1 and cloned in-frame with Green Fluorescence Protein in pEGFP-N2 (Clontech, Mountain View, CA, USA) to generate the intermediate cloning product pEGFP-Cter STAT1. The amino-terminal fragment of STAT1 was released from the MGC-3493 clone by digesting *Bam*H1-*Hind*III and cloned into pEGFP-Cter STAT1 that had been previously digested *Bgl*II-*Hind*III. The final plasmid, containing GFP fused in frame to carboxyl-terminus of STAT1 was confirmed by double stranded sequencing. Before transfection, HT1080 fibrosarcoma cells were plated in 6 well plates at a density of $1x10^5$ cells/well. Cells were transfected with Fugene 6 Transfection Reagent (Roche Diagnostics, Rotkreuz, Switzerland) following the manufacturers' instructions and cultured in the presence of 1 mg/ml geneticin (Life Technologies, Carlsbad, CA, USA) from 24 hr after transfection. Selection was considered complete when all untransfected cells were dead. To assess IFN-α mediated STAT1-GFP nuclear translocation, HT1080 STAT1-GFP cells were seeded at a density of 10'000 cells/well in Packard View-Plate™ 96-well plates (PerkinElmer, Waltham, MA, USA) 16-24 hr prior to the experiment. On the day of assay, the medium was replaced with 90 µl/well of medium containing serial dilutions of the pan-JAK inhibitor tofacitinib or CHZ868 (in duplicates) in the absence of geneticin, and cells were preincubated with inhibitor for 30 min. Cells were then stimulated with, IFN-α (Immunotools, Friesoythe, Germany) added at a final concentration of 100 ng/ml for 30 min at 37°C. After stimulation, the medium was replaced by pre-warmed fixation solution (3.7 % formaldehyde, Amresco, Solon, OH, USA; diluted in PBS) for 10 min and subsequently incubated in DNA-staining solution (Hoechst-33342, Molecular Probes) for 30 s. Nuclear STAT1-GFP translocation was assessed using the Cellomics high content reader (Array Scan® V^{TI}, Thermo Scientific, Waltham, MA, USA). Cells not treated with IFN-α served as controls. The percentage of nuclear STAT1-GFP was determined by plotting background-corrected data in Excel and subsequent calculation of IC_{50} values using XLfit4 (ID Business Solutions Ltd, Surrey, UK).

Supplemental murine models and analysis of mice. For assessment of type I inhibitor persistent cells in vivo, ruxolitinib persistent 32D *MPL*W515L GFP^+ cells were injected into C3H/HeJ mice from which 32D cells were originally derived, at 1.3 x 10^6 cells/mouse via tail vein. Engraftment was documented by flow cytometric analysis for GFP^+ cells in bone marrow aspirates 10 days post injection. Animals were randomized according to bone marrow GFP^+ cells and treated with CHZ868 40 mg/kg qd or vehicle by oral gavage for 2 weeks (n=8-9/group). Effects on spleen and liver weight were assessed at 7 days of treatment as compared

to age-matched controls. Survival of animals was monitored and mice were sacrificed when moribund. Infiltration of bone marrrow, spleen, liver and lung by 32D *MPL*W515L GFP$^+$ cells was assessed by flow cytometric analysis of GFP$^+$ cells or by immunohistochemical staining for GFP at end of life. For quantification of 32D *MPL*W515L GFP$^+$ infiltration, anti-GFP stained immunohistochemistry slides were scanned by a digital scanner (FLASH, PerkinElmer) using a 20X lens (NA.0.8 PL APO) and the area of GFP labeled tissue, as well as the area of the entire tissue was quantified by Metamorph software after color thresholding. Amount of GFP per tissue was calculated by dividing the thresholded GFP area with the area of the entire tissue.

The *Jak2*V617F retroviral bone marrow transplant model was used as described previously(James et al., 2005; Wernig et al., 2006). Efficacy studies and analyses were performed as reported(Evrot et al., 2013; Weigert et al., 2012). Lethally irradiated Balb/c mice were transplanted with *Jak2*V617F-IRES-GFP expressing marrow and randomized to four groups (n=8/group) based on hematocrit. Controls received vehicle, one treatment arm 15 mg/kg CHZ868 orally bid for the first week, and then qd, and the other cohorts CHZ868 at 20 mg/kg or 30 mg/kg qd for 14 days.

Analysis of in vivo apoptosis induction. Apoptosis induction by CHZ868 treatment in vivo was assessed in the *MPL*W515L model by double-immunofluorescence staining for GFP and cleaved Caspase-3 on 3 µm tissue sections of BM (femur) and spleens on the Ventana DISCOVERY ULTRA automated stainer. Antigen retrieval was performed using standard Cell Conditioning 1. Slides were subsequently incubated with primary antibodies against GFP (rabbit polyclonal antibody #598, MBL International Corporation, Woburn, MA, USA) at a dilution of 1:200 and against cleaved Caspase-3 (rabbit polyclonal antibody #9661, Cell Signaling, Danvers, MA, USA) at a dilution of 1:2000. Secondary antibody used was the DISCOVERY OmniMap anti-rabbit HRP (RUO) at a dilution of 1:200. Substrates used for fluorescent detection were the DISCOVERY FITC Kit (RUO) for GFP in green and the DISCOVERY Rhodamine Kit (RUO) for cleaved Caspase-3 in red. The staining for GFP and cleaved Caspase-3 was performed sequentially with a denaturation step at 92 °C for 32 min in between. Nuclei were stained using Hoechst 33342 (Invitrogen) or DRAQ5^{TM} (Alexis Biochemicals). Slides were mounted in Dako Ultramount aqueous permanent mounting medium.
For additional analyses of apoptosis induction by in vivo CHZ868 treatment, CD45.2 *Jak2*V617F C57/B6 bone marrow was mixed 1:1 with CD45.1 *Jak2* WT C57/B6 bone marrow and transplanted into lethally irradiated CD45.1 recipients. Upon disease establishment, mice were randomized according to hematocrit and treated with CHZ868 40 mg/kg or vehicle for 2 days. Harvested bone marrow cells were stained for annexin V positivity using the annexin V PE

apoptosis kit (BD) along with DAPI at 0.5 µg/ml and staining for lineage markers, Sca1, c-Kit, CD45.1 and CD45.2 (eBioscience). Flow cytometric analysis for annexin V positivity in CD45.2 *Jak2*V617F and CD45.1 *Jak2* WT $Lin^-Sca1^-Kit^+$ multipotent myeloid progenitors was performed on LSRFortessa and analyzed by FlowJo software. C57BL/6 mice transplanted with retrovirally transduced *MPL*W515L GFP bone marrow were treated with CHZ868 at 40 mg/kg or vehicle for 10 days analogous to GFP/caspase-3 immunofluorescence in the *MPL*W515L model. Harvested bone marrow was stained for annexin V along with DAPI and for lineage markers, Sca-1 and c-Kit, and annexin V positivity in GFP^+ *MPL*W515L and in GFP^- *MPL* WT $Lin^-Sca1^-Kit^+$ multipotent myeloid progenitors was assessed.

Supplemental References

Jolliffe, I. T. (2002). Principal Component Analysis. In, (New York: Springer).
Law, C. W., Chen, Y., Shi, W., and Smyth, G. K. (2014). voom: precision weights unlock linear model analysis tools for RNA-seq read counts. Genome biology *15*, R29.
Subramanian, A., Tamayo, P., Mootha, V. K., Mukherjee, S., Ebert, B. L., Gillette, M. A., Paulovich, A., Pomeroy, S. L., Golub, T. R., Lander, E. S., and Mesirov, J. P. (2005). Gene set enrichment analysis: a knowledge-based approach for interpreting genome-wide expression profiles. Proceedings of the National Academy of Sciences of the United States of America *102*, 15545-15550.
Wernig, G., Mercher, T., Okabe, R., Levine, R. L., Lee, B. H., and Gilliland, D. G. (2006). Expression of Jak2V617F causes a polycythemia vera-like disease with associated myelofibrosis in a murine bone marrow transplant model. Blood *107*, 4274-4281.